due to their greater inertia. Both separated flow models yield reasonably good predictions of flow properties, except for underestimation of mean particle velocities far from the jet axis. In contrast, predictions using the LHF model overestimate rates of flow development—similar to past experience with this approach.[1-4]

Conclusions

Evaluation of the SSFM model using the measurements of Modarress et al.[5,6] yielded results comparable to earlier work.[3,7] This is encouraging since all model constants (aside from $C_{\epsilon 3}$ whose value is not critical for these measurements) were unchanged from earlier work.[1-4] Present results suggest that data from coflowing jets in ducts should be accompanied by static pressure measurements, since even small pressure gradients appreciably influence jet properties. Furthermore, coflow sufficient for entrainment requirements should be supplied to avoid development of recirculation zones. Evaluation using the same measurements does not suggest any particular advantage of the method proposed by Elghobashi and Abou-Arab.[7] However, the stochastic model proposed by Gosman and Ioannides,[9] and further developed in Refs. 1-4, uses instantaneous flow properties to handle the interactions between turbulence and nonlinear interphase transport with less empiricism; therefore, it has greater potential for treating practical spray evaporation and combustion problems from first principles.[4,8] Development and evaluation of the method are being continued this laboratory.

Acknowledgment

This research was sponsored by National Aeronautics and Space Administration Grant NAG 3-190, under the technical management of R. Tacina of the Lewis Research Center.

References

[1]Shuen, J-S., Chen, L-D., and Faeth, G. M., "Evaluation of a Stochastic Model of Particle Dispersion in a Turbulent Round Jet," *AIChE Journal*, Vol. 29, Jan. 1983, pp. 167-170.

[2]Shuen, J-S., Chen, L-D., and Faeth, G. M., "Predictions of the Structure of Turbulent Particle-Laden Round Jets," *AIAA Journal*, Vol. 21, Nov. 1983, pp. 1483-1484.

[3]Shuen, J-S., Solomon, A.S.P., Zhang, Q-F., and Faeth, G. M., "Structure of Particle-Laden Jets: Measurements and Predictions," AIAA Paper 84-0038, Jan. 1984.

[4]Solomon, A.S.P., Shuen, J-S., Zhang, Q-F., and Faeth, G. M., "Structure of Nonevaporating Sprays: Measurements and Predictions," AIAA Paper 84-0125, Jan. 1984.

[5]Modarress, D., Wuerer, J., and Elghobashi, S., "An Experimental Study of a Turbulent Round Two-Phase Jet," AIAA Paper 82-0964, June 1982.

[6]Modarress, D., Tan, H., and Elghobashi, S., "Two-Component LDA Measurement in a Two-Phase Turbulent Jet," AIAA Paper 83-0052, Jan. 1983.

[7]Elghobashi, S. E. and Abou-Arab, T. W., "A Two-Equation Turbulence Model for Two-Phase Flows," *The Physics of Fluids*, Vol. 26, 1983, pp. 931-938.

[8]Faeth, G. M., "Recent Advances in Modeling Particle Transport Properties and Dispersion in Turbulent Flow," *Proceedings of the ASME-JSME Thermal Engineering Conference*, Vol. 2, March 1983, pp. 517-534.

[9]Gosman, A. D. and Ioannides, E., "Aspects of Computer Simulation of Liquid-Fueled Combustors," AIAA Paper 81-0323, 1981.

[10]Abramovich, G. N., *Theory of Turbulent Jets*, MIT Press, Cambridge, Mass., 1963, pp. 509-511.

[11]Becker, H. A., Hottel, H. C., and Williams, G. C., "Mixing and Flow in Ducted Turbulent Jets," *Ninth Symposium (International) on Combustion*, The Combustion Institute, Pittsburgh, Pa., 1962, pp. 7-20.

[12]Comment of anonymous reviewer, 1984.

Laser Determination of Anisotropic Plasma Electron Density Profiles

Richard C. Warder Jr.*
University of Missouri—Columbia
Columbia, Missouri

In a recent series of papers, Self and colleagues[1-3] have measured the electron concentration in combustion MHD plasmas using submillimeter waves. These studies have utilized submillimeter laser interferometry supplemented by electric probes and more recently have been extended to include Faraday rotation measurements. The data analysis assumes that the plasma electron density is uniform. Annen[2] has investigated the electron density profile using an electric probe with a fixed bias to collect the ion current as the probe was swept to the plasma channel centerline. It is difficult to infer a density profile from the data, due to both the fluctuations in the probe current and the nonlinearity between probe current and electron density ($I \sim n^{3/4}$). This Note indicates how their Faraday rotation experimental arrangement can be used to infer the electron density distribution in the "line-of-sight" direction and also suggests a means for improved data acquisition.

If the plasma is assumed to be uniform over the propagation path, the determination of electron density is straightforward: one simply measures the interferometer fringe shift or the Faraday rotation angle and works backward. In general, the electron density in any physical situation is not uniform. The finite thickness of the plasma and the method by which it is generated will introduce boundary effects and consequently gradients of electron density in the direction of propagation (and possibly orthogonal to that direction as well). Thus, the sensitivity of the measurements to departures from the discrete interface assumption must be taken into consideration. It is this electron density distribution that we shall attempt to infer by an alternative analysis of Faraday rotation data.

Wharton et al.[4,5] devised a method for determining nonmagnetized plasma electron density profiles using an interferometer to measure the phase shift due to the plasma at several microwave probing frequencies. The frequencies are chosen so that, at the lowest one, the wave is just cut off, thereby determining the center or maximum electron density from the condition $\omega = \omega_p$. The phase shifts at the other frequencies are then appropriately normalized and compared with theoretical phase shift curves computed for various assumed electron density distributions. Thus, an estimate of the electron density profile can be obtained. However, the experimental arrangements can become quite complicated because a number of different simultaneous microwave setups are required in order to obtain data at widely separated microwave frequencies.

The results described here have a twofold usefulness. First, they will enable one to infer the electron density profile of a plasma in a magnetic field when the results of Wharton and Slager[4] cannot be used. Second, instead of determining the propagation phenomena as a function of microwave frequency, one can vary the magnetic field strength. Generally, this is more easily done and also allows a wider range of parameters to be covered than when only the laser frequency is changed.

Received July 27, 1984.

*Professor of Mechanical and Aerospace Engineering. Associate Fellow AIAA.

The rotation of the plane of polarization that results when plasma is introduced into the transmission path is given by[5]

$$\theta=\frac{\beta_0}{2}\int_0^d\left[\frac{\beta_+(z)}{\beta_0}-\frac{\beta_-(z)}{\beta_0}\right]dz \tag{1}$$

$$\theta=\frac{\beta_0}{2}\int_0^d\left[1-\frac{n(z)}{n_c(1-\omega_B/\omega)}\right]^{1/2}dz - \frac{\beta_0}{2}\int_0^d\left[1-\frac{n(z)}{n_c(1+\omega_B/\omega)}\right]^{1/2}dz \tag{2}$$

where $n(z)$ is the electron density distribution function that is assumed to be slowly varying compared to a wavelength, n_c the maximum or "cutoff" electron density in the absence of a magnetic field, and all other notation is that of Self,[1-3] except that we have used a phase-constant notation rather than refractive indices.

The numerical integration of Eq. (2) is straightforward. For an assumed cosine and Gaussian distribution with $x=z/d$,

$$\theta'=\frac{2\theta}{\beta_0 d}=\int_0^1\left\{1-\frac{n_p}{n_c}\frac{\cos[(\pi/2)(2x-1)]}{(1-\omega_B/\omega)}\right\}^{1/2}dx - \int_0^1\left\{1-\frac{n_p}{n_c}\frac{\cos[(\pi/2)(2x-1)]}{(1+\omega_B/\omega)}\right\}^{1/2}dx \tag{3}$$

$$\theta'=\frac{2\theta}{\beta_0 d}=\int_0^1\left\{1-\frac{n_p}{n_c}\frac{\exp[-(2x-1)^2]}{1-\omega_B/\omega}\right\}^{1/2}dx - \int_0^1\left\{1-\frac{n_p}{n_c}\frac{\exp[-(2x-1)^2]}{1+\omega_B/\omega}\right\}^{1/2}dx \tag{4}$$

where $\beta_0=2\pi/\lambda$ and n_p corresponds to the peak of the electron density profile and is assumed to be less than n_c.

Equation (2) was integrated for several assumed distributions and some of the results are plotted in Fig. 1. Distributions not shown include parabolic, triangular, cosine, and a "regular" trapezoidal ($b=d/3$). Faraday rotation for a trapezoidal distribution is the sum of the proportionate contributions from a triangular and a uniform contribution. The calculations indicate that it may be difficult to distinguish between the parabolic, cosine, and "regular" trapezoidal distributions or between a triangular and cosine-squared distribution. Wharton's phase shift calculations indicate similar findings.[4,5] Accordingly, we will confine our discussion to the cosine, cosine-squared, and Gaussian distributions.

Consider the largest electron density data of Table 2 of Annen et al.[3] (which assume a uniform distribution). Assume that the actual electron density profile had a cosine variation, then $n_p=(\pi/2)n_{\text{uniform}}$ of Table 2 for the same total rotation angle. Figure 2a shows the rotation angle for the three assumed distributions as a function of magnetic field, assuming a channel width of 7 cm. Figure 2 also shows the results of similar computations assuming that the 496 μm laser source of Ref. 1 was used. Similar computations were also made using the lowest electron density reported for both the 400 and 496 μm laser lines.

Assuming that the experimental error of ± 4.1 deg is constant, it would be possible to readily differentiate between the three 496 μm distributions shown in Fig. 2, but only marginally between the three 400 μm distributions. At the lowest electron density, it would not be feasible to differentiate between the distributions even at 496 μm. However, the improved techniques that have been suggested[3] using a pair of detectors and a polarizing beam splitter should provide significant increases in angular resolution (~ 0.3 deg). This should be adequate to differentiate between the three distributions at the lowest electron density using 400 μm data.

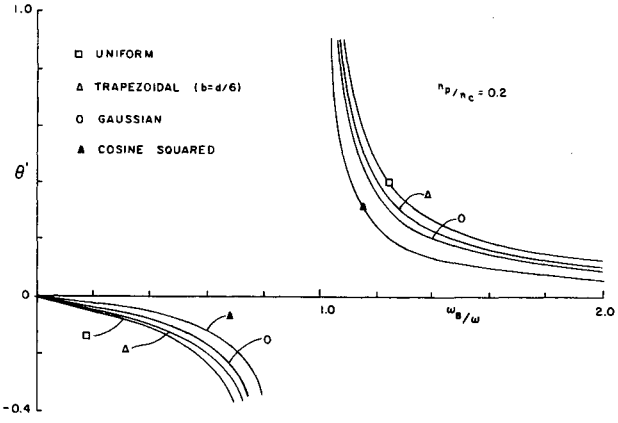

Fig. 1 Normalized Faraday rotation angle as a function of normalized electron cyclotron frequency for selected spatial distributions.

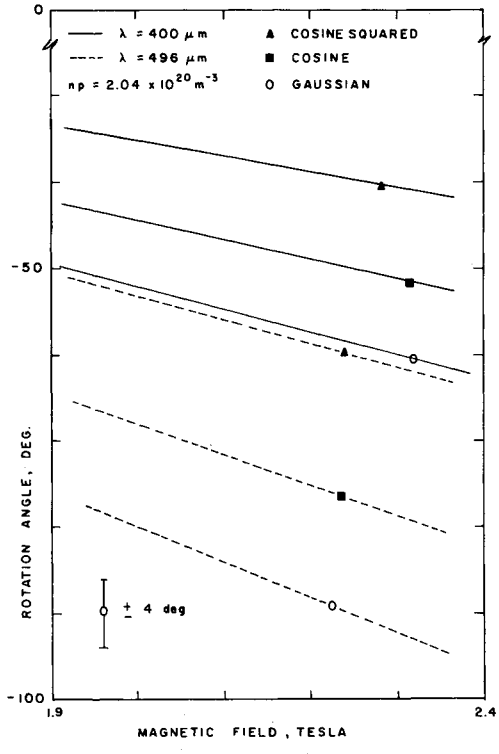

Fig. 2 Total Faraday rotation angle as a function of magnetic field for selected spatial distributions. These curves correspond to the linear region of Fig. 1 as $\omega_B/\omega<0.02$.

An approach that has been previously used in the microwave region[6] utilizes a mechanized continuously rotating "half-wave" plate to generate the curve shown in Fig. 5 of Ref. 3. Comparison of the curves generated with "no plasma" and for the actual operating conditions are used to determine the Faraday rotation angle. Maxima as well as minima can be used. Alternatively, graphical extrapolation of opposite slopes of the response curve into the noise region can be used to locate the midpoint of these intercepts, which are then used to estimate a minimum location.

A key difficulty with the present development is determining the peak electron density in the profile. One can certainly estimate the value by a limited number of measurements. Reduction of the rotation data assuming a uniform profile

and then using the peak corresponding to some assumed profile provides a straightforward starting point. The use of a variable frequency microwave source at a "magnetoplasma resonance cutoff" condition ($\beta_- \to 0$) appears reasonable at least for the electron density conditions given in Table 2 of Ref. 3. Although significant changes in the magnetic field may alter the electron density profile, a 5% field variation should be sufficient for data acquisition.

Finally, spatial variations in the magnetic field as well as those in the electron density as mentioned earlier will influence the data reduction, although known field variations could be included in the integration of Eq. (1).

References

[1]Self, S. A., Reigel, F. O., Clements, R. M., and James, R. K., "Electron Concentration Measurements in Combustion MHD Flows by Submillimeter Laser Interferometry," *Journal of Energy*, Vol. 1, July-Aug. 1977, pp. 206-211.

[2]Annen, K. D., Kuzmenko, P. J., Keating, R., and Self, S. A., "Electron and Positive Ion Measurements in MHD Combustion Plasmas with Phosphorous Addition," *Journal of Energy*, Vol. 5, Jan.-Feb. 1981, pp. 31-38.

[3]Kuzmenko, P. J. and Self, S. A., "Measurement of Plasma Conductivity Using Faraday Rotation of Submillimeter Waves," *Journal of Energy*, Vol. 7, March-April 1983, pp. 176-181.

[4]Wharton, C. B. and Slager, D. M., "Microwave Determination of Plasma Density Profiles," *Journal of Applied Physics*, Vol. 31, 1960, pp. 428-430.

[5]Heald, M. A. and Wharton, C. B., *Plasma Diagnostics with Microwaves*, John Wiley & Sons, New York, 1965.

[6]Warder, R. C. Jr., "Microwave Measurements of Arc-Heated Argon Plasmas," Northwestern University, Evanston, Ill., NU-GDL Rept. B-1-63, April 1963.

Transonic Flow in the Throat Region of Radial or Nearly Radial Supersonic Nozzles

B. F. Carroll* and J. C. Dutton†
Texas A&M University, College Station, Texas

Introduction

IN a recent paper, Conley et al.[1] analyzed annular nozzles using a time-dependent transonic technique to provide a starting line for supersonic method-of-characteristics calculations. Their attempts to analyze geometries for which the radial velocity components were large were hampered by the lack of an adequate transonic solution for the case of highly inclined throat flow. According to Ref. 1, "This inadequacy in predictive capability is identified as a major deficiency in the state-of-the-art of nozzle flowfield analysis." In response to this need, a transonic solution is presented that is applicable to annular nozzles with the throat flow inclined at arbitrary, but large, angles to the nozzle axis of symmetry. This solution is a computationally efficient means of establishing a supersonic initial value line for space-marching supersonic calculations. Both radial inflow and outflow as well as planar geometries may be analyzed with this solution.

Received Aug. 6, 1984.

*ONR Graduate Fellow, Department of Mechanical Engineering. Student Member AIAA.

†Associate Professor, Department of Mechanical Engineering. Member AIAA.

In previous work, Dutton and Addy presented third-order series expansion solutions for transonic flow in axisymmetric nozzles[2] and annular nozzles[3] that showed excellent agreement with experimental measurements. For annular nozzles, the perturbation velocity components were expanded in power series in the parameter ϵ, defined as $\epsilon \equiv 1/(\bar{R}_c + \eta)$, where $\bar{R}_c$ is an average dimensionless wall radius of curvature at the throat and η an arbitrary parameter included to improve the convergence of the series. The inclusion of the parameter η was shown to extend the applicability of the series solution to nozzles with small wall radii of curvature at the throat. However, only annular nozzles with small flow inclination angles could be analyzed, as a result of the order-of-magnitude assumptions made in the problem formulation.

Problem Formulation and Solution

A regular perturbation technique is to be used to obtain an approximate solution to the throat flowfield sketched in Fig. 1. The inclination angle β is measured between the Z axis of symmetry and the main flow x direction and is positive in the counterclockwise direction. The governing equations are taken as the irrotationality condition and the gasdynamic equation; the boundary conditions are that the nozzle walls are streamlines. These equations are transformed from the cylindrical R-Z coordinate system to the local dimensionless x-y system with lengths nondimensionalized by the throat half-height D and velocities by the critical speed of sound a^*. The perturbation velocity components $\tilde{u}$ and $\tilde{v}$ are defined by $u = 1 + \tilde{u}$ and $v = \tilde{v}$. Using the expansion parameter defined by Dutton and Addy[3] and discussed in the introduction, strict order-of-magnitude estimates[4] show that $\tilde{u} = \mathcal{O}(\epsilon)$, $\tilde{v} = \mathcal{O}(\epsilon^{3/2})$, and $x = \mathcal{O}(\epsilon^{1/2})$. In this analysis, $\sin\beta$ was taken as $\mathcal{O}(1)$ and $\cos\beta$ as $\mathcal{O}(\epsilon^{1/2})$, i.e., the radial or nearly radial configuration, $\beta \cong \pm\pi/2$.

Defining a new $\mathcal{O}(1)$ stretched axial coordinate z as

$$z \equiv \left(\frac{2}{\gamma+1}\right)^{1/2} x\epsilon^{-1/2} \tag{1}$$

the appropriate expansions for $\tilde{u}$ and $\tilde{v}$ are

$$\tilde{u}(z,y) = u_1(z,y)\epsilon + u_2(z,y)\epsilon^2 + u_3(z,y)\epsilon^3 + \ldots \tag{2}$$

$$\tilde{v}(z,y) = \left(\frac{\gamma+1}{2}\epsilon\right)^{1/2} [v_1(z,y)\epsilon + v_2(z,y)\epsilon^2 + v_3(z,y)\epsilon^3 + \ldots] \tag{3}$$

where γ is the gas specific heat ratio. Using the order-of-magnitude estimates,[4] all variables are redefined in terms of $\mathcal{O}(1)$ quantities. Equations (2) and (3) along with the $\mathcal{O}(1)$ quantities are then substituted into the governing equations and boundary conditions. The boundary conditions must first be expanded in Taylor series about $y = \pm 1$ and the equations defining the wall contours are also expanded in Maclaurin series about $x = 0$. Coefficients of like powers of ϵ are gathered and equated, resulting in the following formulation for the various solution orders. The irrotationality con-

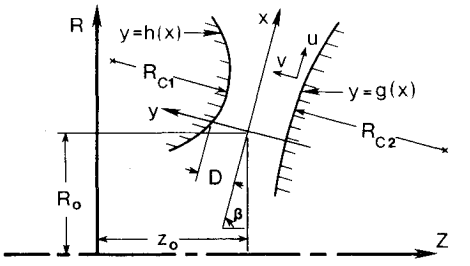

Fig. 1 Schematic of throat flowfield in a radial supersonic nozzle.